Hierarchical Control of Droop-Controlled AC and DC Microgrids—A General Approach Toward Standardization

Josep M. Guerrero, *Senior Member, IEEE*, Juan C. Vasquez, José Matas, Luis García de Vicuña, and Miguel Castilla

***Abstract*—AC and dc microgrids (MGs) are key elements for integrating renewable and distributed energy resources as well as distributed energy-storage systems. In the last several years, efforts toward the standardization of these MGs have been made. In this sense, this paper presents the hierarchical control derived from ISA-95 and electrical dispatching standards to endow smartness and flexibility to MGs. The hierarchical control proposed consists of three levels: 1) The primary control is based on the droop method, including an output-impedance virtual loop; 2) the secondary control allows the restoration of the deviations produced by the primary control; and 3) the tertiary control manages the power flow between the MG and the external electrical distribution system. Results from a hierarchical-controlled MG are provided to show the feasibility of the proposed approach.**

***Index Terms*—Distributed generation (DG), distributed power systems, droop method, hierarchical control, ISA-95, microgrid (MG), parallel operation, smart grid (SG).**

I. Introduction

ELECTRICAL grids tend to be more distributed, intelligent, and flexible. New power-electronic equipment will dominate the electrical grid in the next decades. The trend of this new grid is to become more and more distributed, and hence, energy generation and consumption areas cannot be conceived separately. Nowadays, electrical and energy engineering have to face a new scenario in which small distributed power generators and dispersed energy-storage devices have to be integrated together into the grid. The new electrical grid, also named smart grid (SG), will deliver electricity from suppliers to consumers using digital technology to control appliances at consumers' homes to save energy, thus reducing cost and increasing reliability and transparency. In this sense, the expected whole energy system will be more interactive, intelligent, and distributed. The use of distributed generation (DG) of energy systems makes no sense without using distributed storage systems to cope with the energy balances.

Microgrids (MGs), also named minigrids, are becoming important concepts to integrate DG and energy-storage systems. The concept has been developed to cope with the penetration of renewable-energy systems, which can be realistic if the final user is able to generate, store, control, and manage part of the energy that it will consume. This change of paradigm allows the final user to be not only a consumer but also a part of the grid.

DC and ac MGs have been proposed for different applications, and hybrid solutions have been developed [1]–[12]. Islanded MGs have been used in applications like avionics, automotive, marine, or rural areas. The interfaces between the prime movers and the MGs are often based on power-electronic converters acting as voltage sources (voltage-source inverters (VSI) in case of ac MGs). These power-electronic converters are connected in parallel through the MG. In order to avoid circulating currents among the converters without using any critical communication between them, the droop-control method is often applied.

In the case of parallel inverters, the droop method consists of subtracting proportional parts of the output average active and reactive powers from the frequency and amplitude of each module to emulate virtual inertias. These control loops, also called $P-\omega$ and $Q-E$ droops, have been applied to connect inverters in parallel in uninterruptible power supply (UPS) systems to avoid mutual control wires while obtaining good power sharing. However, although this technique achieves high reliability and flexibility, it has several drawbacks that limit its application.

For instance, the conventional droop method is not suitable when the paralleled system must share nonlinear loads because the control units should take into account harmonic currents and, at the same time, to balance active and reactive power. Thus, harmonic-current-sharing techniques have been proposed to avoid the circulating distortion power when sharing nonlinear loads. All of them consist in distorting the voltage to enhance the harmonic-current-sharing accuracy, resulting in a tradeoff. Recently, novel control loops that adjust the output impedance of the units by adding output virtual reactors [5], [6] or resistors [7] have been included into the droop method, with the purpose of sharing the harmonic-current content properly.

Manuscript received August 10, 2009; revised January 5, 2010, March 10, 2010, and June 9, 2010; accepted July 22, 2010. Date of publication August 12, 2010; date of current version December 10, 2010. This work was supported by the Spanish Ministry of Science and Innovation under Grant ENE2009-13998-C02-01.

J. M. Guerrero and J. C. Vasquez are with the Department of Automatic Control Systems and Computer Engineering, Universitat Politècnica de Catalunya, 08036 Barcelona, Spain (e-mail: josep.m.guerrero@ upc.edu).

J. Matas, L. G. de Vicuña, and M. Castilla, are with the Department of Electronic Engineering, Universitat Politècnica de Catalunya, 08800 Vilanova i la Geltrú, Spain.

Color versions of one or more of the figures in this paper are available online at http://ieeexplore.ieee.org.

Digital Object Identifier 10.1109/TIE.2010.2066534

Further, by using the droop method, the power sharing is affected by the output impedance of the units and the line impedances. Hence, those virtual output-impedance loops can solve this problem. In this sense, the output impedance can be seen as another control variable.

Moreover, another important disadvantage of the droop method is its load-dependent frequency deviation, which implies a phase deviation between the output-voltage frequency of the UPS system and the input voltage provided by the utility mains. This fact can lead to a loss of synchronization since the bypass switch must connect the utility line directly to the MG bus. Consequently, this method, in its original version, can be only applied to islanded MGs [9]. Hence, this technique is not directly applicable to line interactive MGs since the transition between islanded and grid-connected modes will be difficult due to loss of synchronization. In addition, the inherent tradeoff of this method between frequency and amplitude regulation in front of active- and reactive-power sharing accuracy cannot be avoided in islanded mode [14]–[19]. Significant efforts have been done to improve the droop-control method to avoid the aforementioned frequency deviation. In [12], a local controller shifts up the droop function to restore the initial frequency of the inverters by using an integrator to avoid frequency deviation. However, in practical situations when the inverters are not connected to the ac-bus at the same time, the integrator initial conditions are different, and, as a consequence, power sharing is degraded.

Another possibility is to wait for accidental synchronization, taking advantage of the fact that the mains and the MG frequencies are not exactly equal; hence, the phase of the MG drifts gradually toward the mains phase. Thus, the bypass switch can be closed when the two phases match. However, it is hazardous and can take a lot of time. Further, the transient at the time of reclosing can be uneven since the frequencies may not have matched. To overcome this problem, an inverter can be located physically near the bypass switch. This inverter can then be synchronized with the mains grid for seamless reconnection. However, during the synchronization process, this inverter will be overloaded if there are important number of inverters supplying the MG. As a conclusion, the reliability of these methods is considerably low, and they are definitively not practical. Thus, the use of communications seems unavoidable, it being desirable to be implemented together with the DG for a low-bandwidth noncritical communication system.

On the other hand, in case of paralleling dc power converters, the droop method consists of subtracting a proportional part of the output current from the output voltage reference of each module. Thus, a virtual output resistance can be implemented through this control loop. This loop, also called adaptive voltage position, has been applied to improve the transient response of the voltage-regulation modules in low-voltage high-current applications. In addition, the droop method has also an inherent tradeoff between the voltage regulation and the current sharing between the converters [8]–[13].

To cope with this problem, an external control loop, named secondary control, has been proposed to restore the nominal values of the voltage inside the MG. Further, additional tertiary control can be used to bidirectionally control the power flow when the MG is connected to a stiff power source or the mains (in case of ac MGs) [14]. Hierarchical control applied to power dispatching in ac power systems is well known, and it has been used extensively for decades. Nowadays, these concepts are starting to be applied to wind-power parks and were proposed for isolated photovoltaic (PV) systems. However, with the rise of power-electronic-based MGs, which are able to operate both in grid-connected and in island mode, hierarchical control and energy-management systems are necessary. Some authors proposed secondary [33]–[36] and tertiary controllers [37], [38]. The main problem to be solved in such works is the frequency control of the system. However, voltage stability and synchronization issues are also important to achieve enough flexibility to operate in both modes. Only a few works conceived the MG as a whole problem, taking into account the different control levels.

MGs can be conceived to use dc or ac voltage in the local grid. Also, there are ac sources or MGs interconnected by means of power-electronic interfaces to a dc MG. Thus, hybrids dc–ac MGs are often implemented, being necessary to control the power flow between dc and ac parts. In this sense, it seems reasonable that the dc MG area can be connected to energy-storage systems like batteries, supercapacitors, or hydrogen-based fuel cells. Although dc transmission and distribution systems for high-voltage applications are well established and there is a notable increase of dc MG projects, we cannot find so many studies about the overall control of these systems.

In this paper, we propose a general hierarchical multilevel control for ac and dc MGs. This paper is organized as follows. In Section II, a general approach of the hierarchical control stemming from the ISA-95 is adapted to MGs. In Section III, the hierarchical control is applied to ac MGs, solving the tradeoff of the droop method by implementing a secondary control loop and capable of operating in grid-connected and islanded modes. In Section IV, the approach is applied over a dc MG consisting of droop-controlled converters, which are able to share the load together with a stiff dc source, which can be a dc generator, a dc distribution grid, or rectified ac grid. Finally, Section V gives the conclusions and the future trends toward SGs.

II. General Approach of Hierarchical Control of MGs

The need for standards in MG control is related to the new grid codes that are expected to appear in the future. In this sense, ANSI/ISA-95, or ISA-95, as it is more commonly referred to, is an international standard for developing an automated interface between enterprise and control systems. This standard has been developed for global manufacturers to be applied in all industries and in all sorts of processes, like batch, continuous, and repetitive processes. The objectives of ISA-95 are to provide consistent terminology that is a foundation for supplier and manufacturer communications, to provide consistent information models, and to provide consistent operation models which are the foundation for clarifying application functionality and how information is to be used. In

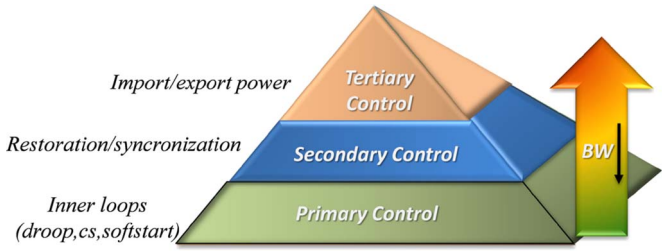

Fig. 1. Hierarchical control levels of an MG.

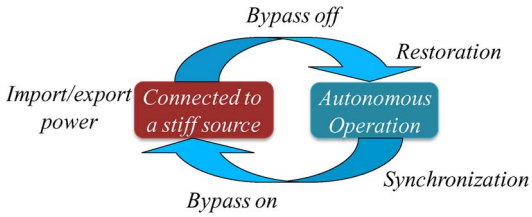

Fig. 2. Stiff-source connection and autonomous operations.

this standard, a multilevel hierarchical control is proposed with the following levels [25], [26].

Level 5: Enterprise. The enterprise level comprises the superior management policies of a commercial entity. This level has operational and developmental responsibility for the entire enterprise, including all of its plants and their respective production lines.

Level 4: Campus/Plant. The campus or plant level comprises superior management policies of a branch or operational division of an enterprise, usually including the elements of the enterprise financial section that are directly associated with that business entity.

Level 3: Building/Production. The building or production level comprises the management and control policies required to administer the states and behaviors of a building and its environmental and production systems.

Level 2: Area/Line. The area or production line level comprises the management and control policies required to administer states and behaviors of a specific area or production line.

Level 1: Unit/Cell. The unit or cell level comprises the management and control policies required to govern the states and behaviors of a unit of automation or a manufacturing cell.

Level 0: Device. The device level comprises the set of field devices that sense and provide actuation of physical processes within the environmental and production systems.

Each level has the duty of a command level and provides supervisory control over lower-level systems. In this sense, it is necessary to ensure that the command and reference signals from one level to the lower levels will have low impact in the stability and robustness performance. Thus, the bandwidth must be decreased with an increase in the control level.

In order to adapt ISA-95 to the control of an MG, zero to three levels can be adopted as follows (see Fig. 1) [7], [14].

1) Level 3 (*tertiary control*): This energy-production level controls the power flow between the MG and the grid.
2) Level 2 (*secondary control*): Ensures that the electrical levels into the MG are within the required values. In addition, it can include a synchronization control loop to seamlessly connect or disconnect the MG to or from the distribution system (see Fig. 2).
3) Level 1 (*primary control*): The droop-control method is often used in this level to emulate physical behaviors that makes the system stable and more damped. It can include a virtual impedance control loop to emulate physical output impedance.
4) Level 0 (inner control loops): Regulation issues of each module are integrated in this level. Current and voltage, feedback and feedforward, and linear and nonlinear control loops can be performed to regulate the output voltage and to control the current while maintaining the system stable.

On the other hand, ac MGs should be able to operate both in grid-connected and islanded modes [27]. The bypass switch is responsible for connecting the MG to the grid. This bypass switch is designed to meet grid-interconnection standards, e.g., IEEE 1547 and UL 1541 in the U.S. Now, the IEEE P1547.4 *Draft Guide for Design, Operation, and Integration of Distributed Resource Island Systems with Electric Power Systems* is in a draft form [28]. It will cover MGs and intentional islands that contain distributed energy resources with utility electric-power systems. The draft provides alternative approaches for the design, integration, and operation of MGs and includes the ability of connection and disconnection to/from the grid.

In grid-connected mode, the MG operates according to IEEE 1547-2003. The transition to islanded mode is done by intentional or unintentional events, e.g., grid failures. Thus, proper islanding-detection algorithms must be implemented. In islanded mode, the MG must supply the required active and reactive powers as well as provide frequency stability and operate within the specified voltage ranges. Reconnection of the MG to the grid will be done when the grid voltage is within acceptable limits and the phasing is correct. Active synchronization is required to match the voltage, frequency, and phase angle of the MG.

III. Hierarchical Control of AC-MGs

AC MGs are now in the cutting edge of the state of the art [20]–[25]. However, the control and management of such a system need still further investigation. MGs for standalone and grid-connected applications have been considered in the past as separate approaches. Nevertheless, nowadays, it is necessary to conceive flexible MGs that are able to operate in both grid-connected and islanded modes. Thus, the study of topologies, architectures, planning, and configurations of MGs are necessary. This is a great challenge due to the need of integrating different technologies of power electronics, telecommunications, generation, and energy-storage systems, among others. In addition, islanding-detection algorithms for MGs are necessary for ensuring a smooth transition between grid-connected and islanded modes. Furthermore, security issues such as fault monitoring, predictive maintenance, or protection are very important regarding MG feasibility.

This section deals with the hierarchical control of ac MGs consisting of the same three control levels as presented in the

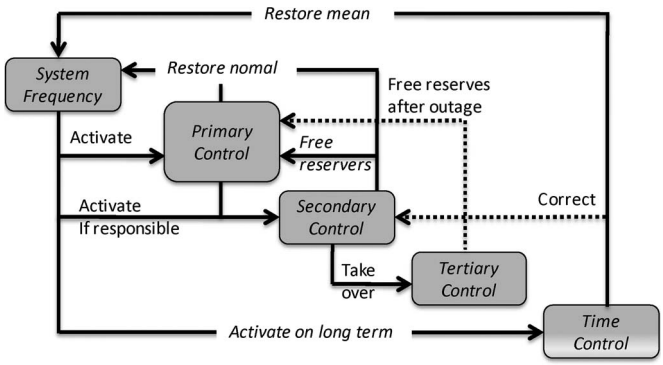

Fig. 3. Frame for the multilevel control of a power system as defined by UCTE.

previous section. The Union for the Co-ordination of Transmission of Electricity (UCTE), Continental Europe, has defined a hierarchical control for large power systems, as shown in Fig. 3. Such a kind of system is supposed to operate over large synchronous machines with high inertias and inductive networks. However, in power-electronic-based MGs, there are no inertias, and the nature of the networks is mainly resistive. Consequently, there are important differences between both systems that we have to take into account when designing their control schemes. This three-level hierarchical control is organized as follows. The primary control deals with the inner control of the DG units, adding virtual inertias and controlling their output impedances. The secondary control is conceived to restore the frequency and amplitude deviations produced inside the MG by the virtual inertias and output virtual impedances. The tertiary control regulates the power flow between the grid and the MG at the point of common coupling (PCC).

A. Inner Control Loops

The use of intelligent power interfaces between the electrical generation sources and the MG is mandatory. These interfaces have a final stage consisting of dc/ac inverters, which can be classified as current-source inverters (CSIs), which consist of an inner current loop and a phase-locked loop (PLL) to continuously stay synchronized with the grid, and VSIs, consisting of an inner current loop and an external voltage loop. In order to inject current to the grid, CSIs are commonly used, while in island or autonomous operation, VSIs are needed to keep the voltage stable.

VSIs are very interesting for MG applications since they do not need any external reference to stay synchronized. Furthermore, VSIs are convenient since they can provide performances like ride-through capability and power-quality enhancement to distributed power generation systems. When these inverters are required to operate in grid-connected mode, they often change their behavior from voltage to current sources. Nevertheless, to achieve flexible MG, i.e., to be able to operate in both grid-connected and islanded modes, VSIs are required to control the exported or imported power to the mains grid and to stabilize the MG [14].

VSIs and CSIs can operate together in an MG. The VSIs are often connected to energy-storage devices, fixing the frequency

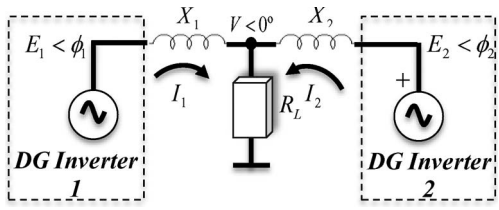

Fig. 4. Equivalent circuit of two parallel-connected inverters.

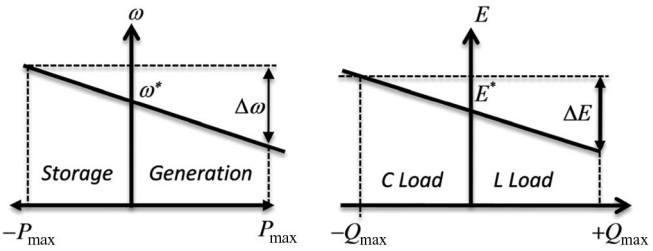

Fig. 5. P/Q droop functions.

and voltage inside the MG. The CSIs are often connected to a PV or small wind turbines (WTs) that require maximum power point tracking algorithms, although those DG inverters could also work as VSIs if necessary. Thus, we can have a number of VSIs and CSIs, or only VSIs, connected in parallel, forming an MG.

B. Primary Control

When connecting two or more VSIs in parallel, circulating active and reactive power can appear (see Fig. 4). This control level adjusts the frequency and amplitude of the voltage reference provided to the inner current and voltage control loops. The main idea of this control level is to mimic the behavior of a synchronous generator, which reduces the frequency when the active power increases [30]. This principle can be integrated in VSIs by using the well-known P/Q droop method [31]

$$\omega = \omega^* - G_P(s) \cdot (P - P^*) \tag{1}$$

$$E = E^* - G_Q(s) \cdot (Q - Q^*) \tag{2}$$

with ω and E being the frequency and amplitude of the output-voltage reference, ω^* and E^* being their references, P and Q as the active and reactive power, P^* and Q^* as their references, and $G_P(s)$ and $G_Q(s)$ as their corresponding transfer functions (typically proportional droop terms as shown in Fig. 5, i.e., $G_P(s) = m$, and $G_Q(s) = n$). Note that the use of pure integrators is not allowed when the MG is in islanded mode since the total load will not coincide with the total injected power, but they can be useful in grid-connected mode to have a good accuracy of the injected active and reactive power [14]. Nevertheless, this control objective will be achieved by the tertiary control level.

The design of $G_P(s)$ and $G_Q(s)$ compensators can be done by using different control-synthesis techniques. However, the dc gain of such compensators (named m and n) provide for the static $\Delta P/\Delta\omega$ and $\Delta Q/\Delta V$ deviations, which are necessary to

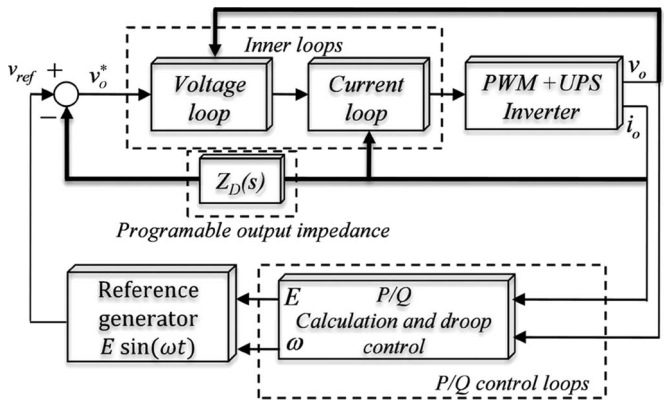

Fig. 6. Virtual-impedance loop.

keep the system synchronized and within the voltage-stability limits. Those parameters can be designed as follows:

$$m = \Delta\omega / P_{\max} \tag{3}$$

$$n = \Delta V / 2Q_{\max} \tag{4}$$

with $\Delta\omega$ and ΔV being the maximum frequency and voltage allowed and $P_{\max}$ and $Q_{\max}$ are the maximum active and reactive power delivered by the inverter. If the inverter can absorb active power, since it is able to charge batteries like a line-interactive UPS, then $m = \Delta\omega / 2P_{\max}$.

Further, the primary control can be used to balance the energy between the DG units and energy-storage elements, e.g., batteries. In this situation, depending on the state of charge (SoC) of the batteries, the contribution of active power can be adjusted according to the availability of energy from each DG unit. Thus, the frequency-droop function can be expressed as

$$\omega = \omega^* - \frac{m}{\alpha} \cdot (P - P^*) \tag{5}$$

with m being the frequency-droop coefficient and α is the per-unit level of charge of the batteries ($\alpha = 1$ is fully charged and $\alpha = 0.01$ is empty). The coefficient α is saturated to prevent $G_P(s)$ from rising to an infinite value. In this way, the DG units will provide energy that is proportional to the batteries' SoC.

In the conventional droop method used by large power systems, it is supposed that the output impedance of synchronous generators, as well as the line impedance, is mainly inductive. However, when using power electronics, the output impedance will depend on the control strategy used by the inner control loops (level 0). Further, the line impedance in low-voltage applications is nearly pure resistive. Thus, the control droops (1), (2) can be modified according to Park's transformation determined by the impedance angle θ

$$\omega = \omega^* - G_P(s)\left[(P - P^*)\sin\theta - (Q - Q^*)\cos\theta\right] \tag{6}$$

$$E = E^* - G_Q(s)\left[(P - P^*)\cos\theta + (Q - Q^*)\sin\theta\right]. \tag{7}$$

The primary-control level can also include the virtual output-impedance loop in which the output voltage can be expressed as [17]

$$v_o^* = v_{\text{ref}} - Z_D(s) \cdot i_o \tag{8}$$

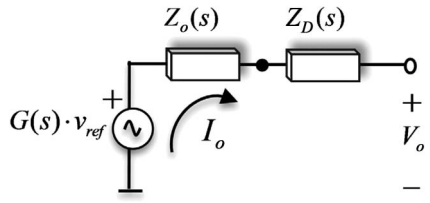

Fig. 7. Equivalent circuit of an inverter with the output-impedance loop.

where v_{ref} is the voltage reference generated by (6) and (7) with $v_{\text{ref}} = E\sin(\omega t)$, and $Z_D(s)$ is the virtual output-impedance transfer function, which normally ensures inductive behavior at the line frequency. Fig. 6 shows the virtual impedance loop in relation with the other control loops: inner current and voltage loops and the droop control. Fig. 7 shows the Thévenin equivalent circuit of an inverter with the virtual impedance [47], which consists of a controlled voltage source $G(s)v_{\text{ref}}$, with $G(s)$ being the closed-loop voltage gain transfer function, connected to the *MG* trough the closed loop output impedance Z_o and the virtual impedance Z_D. Usually, Z_D is designed to be bigger than Z_o; in this way, the total equivalent output impedance is mainly dominated by Z_D [17]. The virtual output impedance Z_D is equivalent to the series impedance of a synchronous generator. However, although the series impedance of a synchronous generator is mainly inductive, the virtual impedance can be chosen arbitrarily. In contrast with a physical impedance, this virtual output impedance has no power losses; thus, it is possible to implement resistance without efficiency losses.

Notice that, by using the virtual-impedance control loop, the inverter output impedance becomes a new control variable. Thus, we can adjust the phase angle of (6) and (7) according to the expected X/R ratio of the line impedance $\theta = \tan^{-1} X/R$ and the angle of the output impedance at the line frequency. Furthermore, the virtual output impedance can provide additional features to the inverter, such as hot-swap operation and harmonic-current sharing.

When connecting a DG unit to the MG, there are unavoidable small differences in phase and/or amplitude that result in current spikes which can damage or overload the unit. For instance, in large WTs, the output impedance of the generator is increased by using external resistors and thyristors and gradually reducing the output impedance, as shown in Fig. 8(a) [45]. In our case, we can implement a similar soft starter by properly changing the value of the virtual impedance. As shown in Fig. 8(b), hot-swap operation can be obtained, as expressed by

$$Z_D(t) = Z_f - (Z_f - Z_i)e^{-t/T} \tag{9}$$

where Z_i and Z_f are the initial and the final virtual impedance values, respectively, and T is the time constant of the start-up process.

On the other hand, by using a bank of bandpass filters, we can independently adjust the output impedance as "seen" by the fundamental and the current harmonics. In this way, we can cope with the tradeoff between the current harmonic sharing

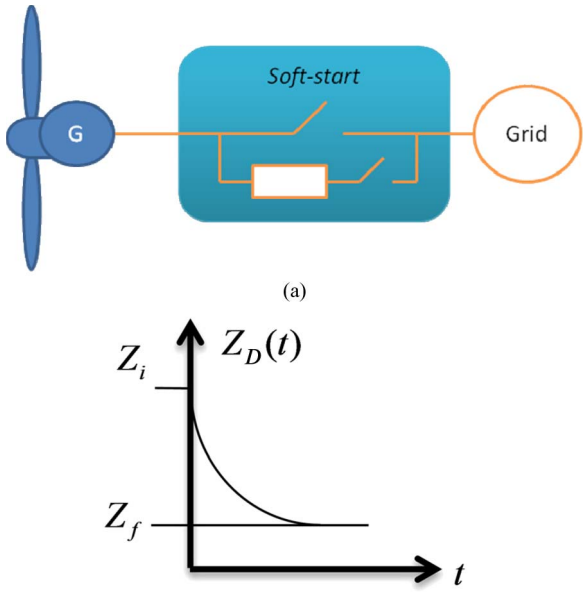

Fig. 8. Soft-start operation. (a) Physical soft starter and (b) operation of the virtual impedance.

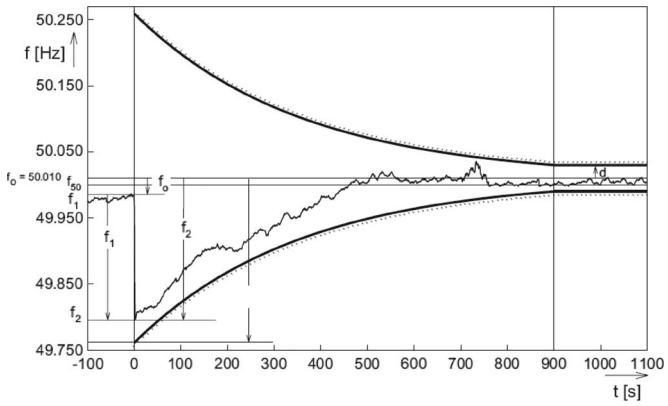

Fig. 9. Frequency-control restoration achieved by the secondary-control action.

and the voltage total harmonic distortion. Thus, the virtual impedance can be expressed as follows:

$$Z_D(s) = L_D \frac{2k_1 s^2}{s^2 + 2\xi\omega_1 s + \omega_1^2} + \sum_{\substack{i=1 \\ \text{odd}}}^{n} R_i \frac{2k_i s}{s^2 + 2\xi\omega_o s + \omega_o^2} \tag{10}$$

where L_D and R_i are the inductive and resistive impedance values, respectively, and k_i is the coefficient of the filter for every harmonic i term. The output impedance can also be designed by taking into account not only the power rating of the inverter but also the voltage drop by this loop and the amplitude droop loop (7).

These control loops allow parallel operation of the inverters. However, these have an inherent tradeoff between P/Q sharing and frequency/amplitude regulation (see Fig. 9) [48]–[51]. Figs. 10 and 11 show the experimental results of the current and voltage waveforms of two inverters sharing a common 7.5-kW resistive load. Notice the good current sharing obtained due to the use of the primary control.

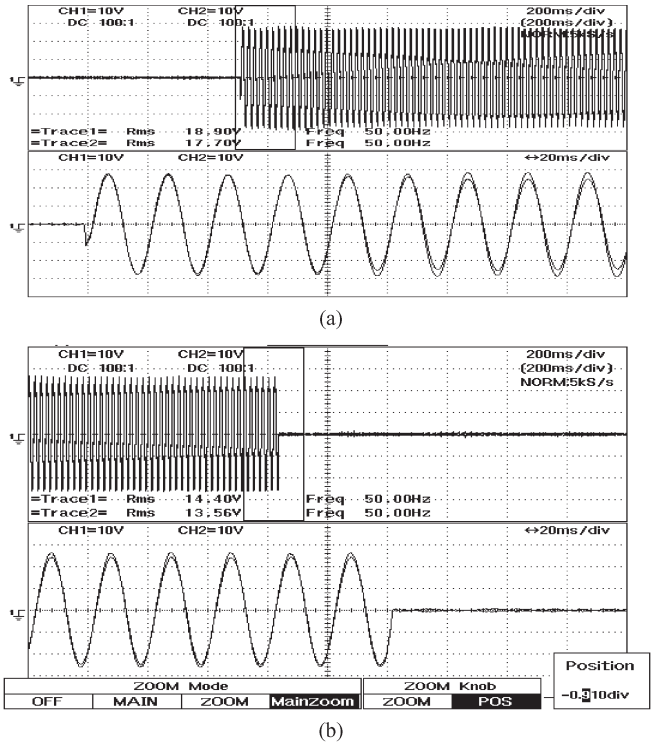

Fig. 10. Current waveforms of two-inverter MG for load step changes (a) from no load to 7.5 kW and (b) back to no load.

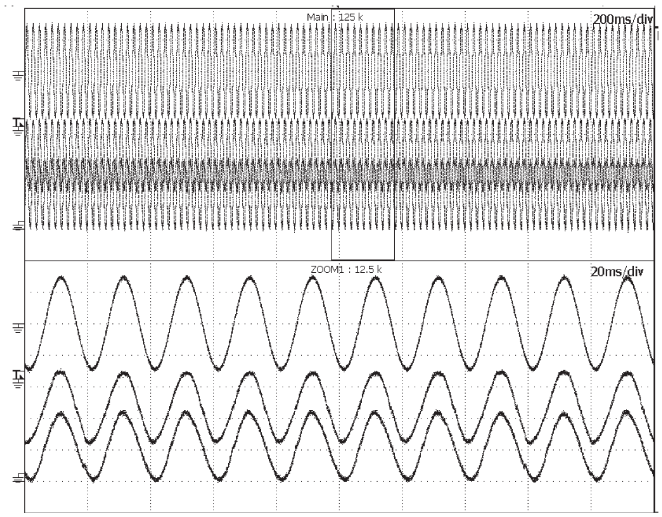

Fig. 11. Waveforms of the parallel system sharing a linear load. (Top) Output voltage and (middle and bottom) load currents.

C. Secondary Control

In order to compensate for the frequency and amplitude deviations, a secondary control is proposed. The secondary control ensures that the frequency and voltage deviations are regulated toward zero after every change of load or generation inside the MG [32]–[35]. The frequency and amplitude levels in the MG, $\omega_{\rm MG}$ and $E_{\rm MG}$, are sensed and compared with the references $\omega^*_{\rm MG}$ and $E^*_{\rm MG}$; the errors processed through the compensators ($\delta\omega$ and δE) are sent to all the units to restore the output-voltage frequency and amplitude.

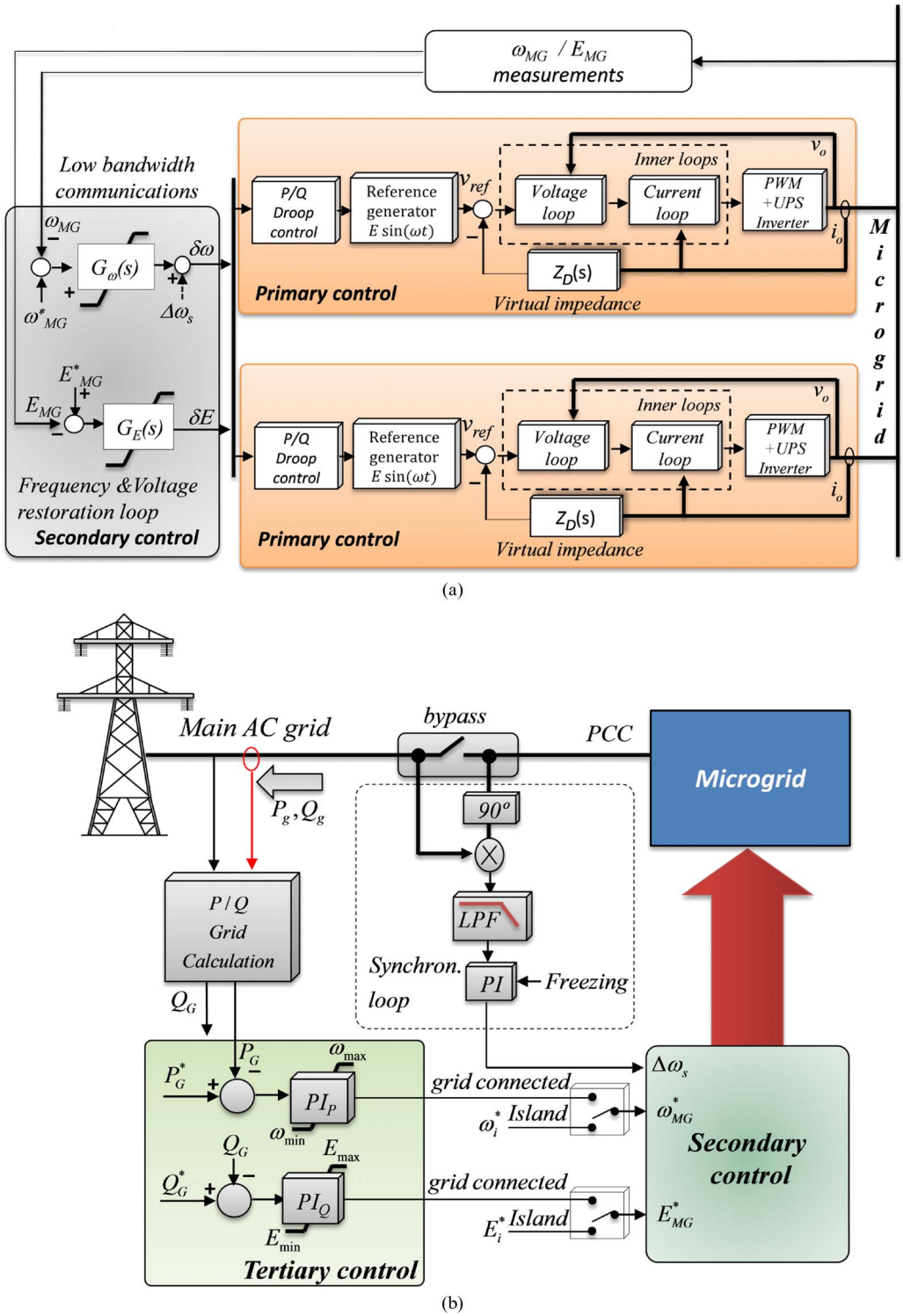

Fig. 12. Block diagrams of the hierarchical control of an ac MG. (a) Primary and secondary controls of an ac MG. (b) Tertiary control and synchronization loop of an ac MG.

Taking into account grid exigencies [7], the secondary control should correct the frequency deviation within allowable limit, e.g., ±0.1 Hz in Nordel (North of Europe) or ±0.2 Hz in UCTE (Continental Europe). It is defined as

$$\delta P = -\beta \cdot G - \frac{1}{T_r}\int G dt \tag{11}$$

where δP is the output set point of the secondary controller, β is the gain of the proportional controller, T_r is the time constant of the secondary controller, and G is the area control error (ACE), which is normally calculated in about 5- to 10-s intervals by computers in the dispatch center as

$$G = P_{\text{meas}} - P_{\text{sched}} + K_{ri}(f_{\text{meas}} - f_0) \tag{12}$$

with P_{meas} being the sum of the instantaneous measured active power transferred at the PCC, P_{prog} being the resulting exchange program, K_{ri} being the proportional factor of the control area set on the secondary controller, and $f_{\text{meas}} - f_0$ being the difference between the instantaneous measured system frequency and the set-point frequency. From (11), note that the control action δP is increased by the integral formula if the deviation of ACE remains constant (proportional–integral (PI)-type controller). This controller is also called load–frequency control or automatic gain controller in the U.S. Fig. 9 shows the experimental results of the restoration process of the grid frequency by using the secondary control.

In case of an ac MG, the frequency and amplitude restoration controllers G_ω and G_E, shown in Fig. 12(a), can be obtained similarly as follows [14]:

$$\delta\omega = k_{p\omega}\left(\omega^*_{\text{MG}} - \omega_{\text{MG}}\right) + k_{i\omega}\int\left(\omega^*_{\text{MG}} - \omega_{\text{MG}}\right)dt + \Delta\omega_S \tag{13}$$

$$\delta E = k_{pE}\left(E^*_{\text{MG}} - E_{\text{MG}}\right) + k_{iE}\int\left(E^*_{\text{MG}} - E_{\text{MG}}\right)dt \tag{14}$$

where $k_{p\omega}$, $k_{i\omega}$, k_{pE}, and k_{iE} are the control parameters of the secondary-control compensator and $\Delta\omega_S$ is a synchronization term which remains equal to zero when the grid is not present. In this case, $\delta\omega$ and δE must be limited in order not to exceed the maximum allowed frequency and amplitude deviations. Fig. 10(a) shows the block diagram of the primary and the secondary control loops of an ac MG. The primary control is only based on local measurements of the output voltage and current to calculate P and Q for the droop method and the virtual impedance control loop. The secondary control will be implemented by an external centralized controller that uses (13) and (14) to restore the deviations produced by the primary control.

In order to connect the MG to the grid, we have to measure the frequency and voltage of the grid, and that will be the reference of the secondary control loop. The phase between the grid and the MG will be synchronized by means of the synchronization control loop shown in Fig. 12(b), which can be seen as a conventional PLL. The output signal of the PLL $\Delta\omega_S$ will be added to the secondary control [see (13)] and will be sent to all the modules to synchronize the MG phase. After several line cycles, the synchronization process will have finished and the MG can be connected to the mains through the static bypass switch. At that moment, the MG does not have any exchange of power with the mains.

Fig. 13(a) shows the synchronization process of the MG with the grid. It can be seen that when the voltage error is small enough, we can swap to the grid-connected operation mode. Fig. 13(b) shows a nonplanned islanding scenario, leading the MG to operate out of synchronization.

D. Tertiary Control

When the MG is operating in grid-connected mode, the power flow can be controlled by adjusting the frequency (changing the phase in steady state) and amplitude of the voltage inside the MG [36]–[38]. As can be seen in the tertiary-control block diagram of Fig. 12(b), by measuring the P/Q through the static bypass switch, P_G and Q_G can be compared with the desired P^*_G and Q^*_G. The control laws PI_P and PI_Q, shown in Fig. 10(b), can be expressed as in the following [14]:

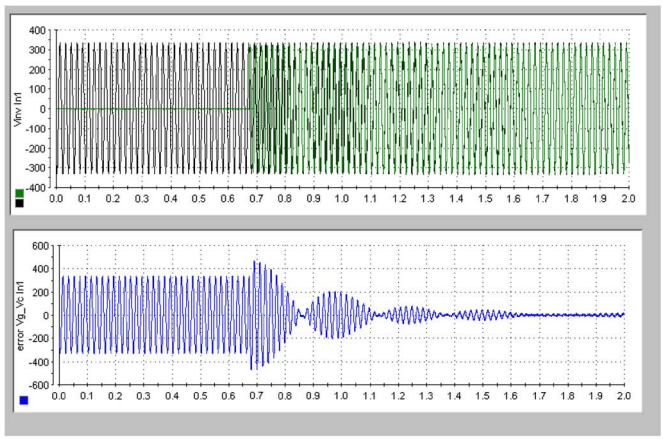

Fig. 13. MG transition modes: (a) Synchronization process. Top: Grid and MG voltages, bottom: voltage difference. (b) Transfer from grid-connected to island mode. Top: Grid and MG voltages, middle: voltage difference and current grid, bottom: active and reactive power injected to the PCC.

$$\omega^*_{\text{MG}} = k_{pP}\left(P^*_G - P_G\right) + k_{iP}\int\left(P^*_G - P_G\right)dt \tag{15}$$

$$E^*_{\text{MG}} = k_{pQ}\left(Q^*_G - Q_G\right) + k_{iQ}\int\left(Q^*_G - Q_G\right)dt \tag{16}$$

with k_{pP}, k_{iP}, k_{pP}, and k_{iQ} being the control parameters of the tertiary-control compensator. Here, ω^*_{MG} and E^*_{MG} are also saturated in case of being outside of the allowed limits. These variables are inner generated in island mode ($\omega^*_{\text{MG}} = \omega^*_i$ and $E^*_{\text{MG}} = E^*_{MG}$) by the secondary control. When the grid is present, the synchronization process can start, and ω^*_{MG} and E^*_{MG} can be equal to those measured in the grid. Thus, the frequency and amplitude references of the MG will be the

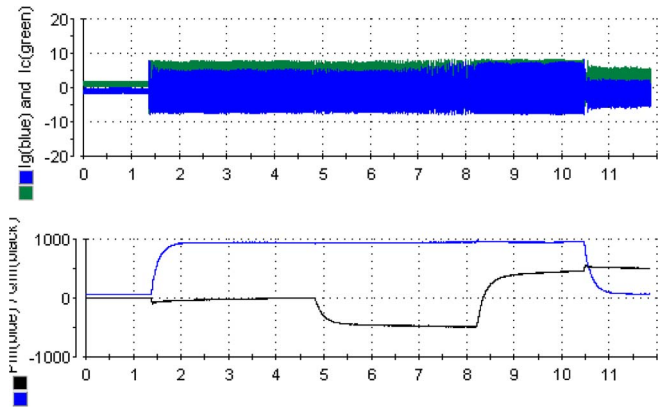

Fig. 14. Experimental results. (a) Currents at the PCC and at the MG load. (b) Active and reactive power injected to the grid.

frequency and amplitude of the mains grid. After the synchronization, these signals can be given by the tertiary control (15) and (16). Notice that, depending on the sign of P_G^* and Q_G^*, the active and reactive power flows can be exported or imported independently.

Note that by making k_{iP} and k_{iQ} equal to zero, the tertiary control will act as a primary control of the MG, thus allowing the interconnection of multiple MGs, forming a cluster.

This control loop can also be used to improve the power quality at the *PCC*. In order to achieve voltage-dip ride through, the MG must inject reactive power to the grid, thus achieving inner voltage stability. Islanding detection is also necessary to disconnect the MG from the grid and disconnect both the tertiary-control references as well as the integral terms of the reactive power PI controllers, to avoid voltage instabilities.

Experimental results were done by using an MG laboratory with a DG generator working as VSI. The MG was able to operate in islanded mode as well as in grid-connected mode.

Fig. 13(a) shows the synchronization process of the MG with the grid. After the MG is completely synchronized, it can be connected to the grid and command P and Q. Since the MG is based on VSIs, if there is some nonplanned grid disconnection, the MG can remain working as an island. Fig. 13(b) shows the transfer from grid-connected to island mode.

Fig. 14 shows the experimental waveforms of the current P and Q injected to the grid. At 1.2 s, the MG was connected to the grid, and the tertiary control started. At this point, we changed the P^* and Q^* as follows. First, we started with $P^* = 1$ kW and $Q^* = 0$ var, injecting real power to the grid and achieving unity power factor. At $t = 4.8$ s, we changed the Q^* from 0 to -500 var, and hence, the MG was acting like a capacitor. Then, at 9.2 s, we suddenly changed Q^* from -500 to $+500$ var; this time, the MG was acting like an inductor. Finally, at $t = 10.5$ s, P^* was fixed to zero without changing the reactive power.

E. Results

Some simulation results from a three-inverter MG are presented. The inverters consisted of a full bridge with an LC filter, rated at 5 kVA. The local controller consisted of current and voltage loops, the P and Q calculations, and the droop control with a virtual output impedance of 50 μH. In this example, the ac MG hierarchical control bandwidth of level 0 is 5 kHz for the voltage control loop and 20 kHz for the current control loop. The bandwidth for levels 1 and 2 are 30 Hz and 3 Hz, respectively. The selected control parameters are listed in Table I.

TABLE I
AC MG CONTROL-SYSTEM PARAMETERS

Parameter	Symbol	Value	Units
Power stage			
Grid Voltage	V_g	311	V
Grid Frequency	f	50	Hz
Grid Inductance	Lg	1e-3	H
Grid Resistance	Rg	1	Ω
Loss resistance inverter I	R_{loss1}	0.1	Ω
Loss resistance inverter II	R_{loss2}	0.11	Ω
Loss resistance inverter III	R_{loss3}	0.09	Ω
Inverter I Inductance	L_1	50e-3	H
Inverter II inductance	L_2	55e-3	H
Inverter III inductance	L_3	45e-3	H
Inverter I resistance	r_1	0.1	Ω
Inverter II inductance	r_2	0.15	Ω
Inverter III inductance	r_3	0.05	Ω
Load	R_L	25	Ω
Primary Control			
Derivative frequency droop	m_d	0.0001	W/rd
Proportional frequency droop	m_p	0.0015	Ws/rd
Proportional amplitude droop	n_p	0.001	VAr/V
Secondary Control			
Proportional frequency droop	k_{pw}	1	Ws/rd
Integral frequency droop	k_{iw}	10	W/rd
Proportional amplitude droop	k_{pE}	1	VAr/V
Integral amplitude droop	k_{iE}	100	VAr·s/V
Tertiary Control			
Proportional phase term	k_{pP}	1e-5	Ws/rd
Integral phase term	k_{iP}	0.1	W/rd
Proportional amplitude term	k_{pQ}	1	W/rd·s
Integral amplitude term	k_{iQ}	100	VAr·s/V

Fig. 15(a) and (b) shows, respectively, the active power and reactive sharing dynamics of the MG system. First, the three-inverter system connected to the grid was started up. The grid reference was fixed from 0 to 1 kW at $t = 2.5$ s by the tertiary control, while the three inverters gave 650 W each. At $t = 2.5$ s, a preplanned islanding scenario occurred, and the grid was disconnected from the MG, operating in autonomous (islanded) operation. Afterward, at $t = 5$ s, one inverter (DG#1) was disconnected suddenly from the grid, and inverters DG#2 and DG#3 provided the power to the local loads. At $t = 7.5$ s, inverter DG#2 was disconnected; thus, inverter DG#3 is supplying all the required power. Notice the flexible operation of the MG, which was able to operate both in grid-connected and in islanded modes.

During the islanded mode, the primary control produces frequency and amplitude deviations, which can be compensated

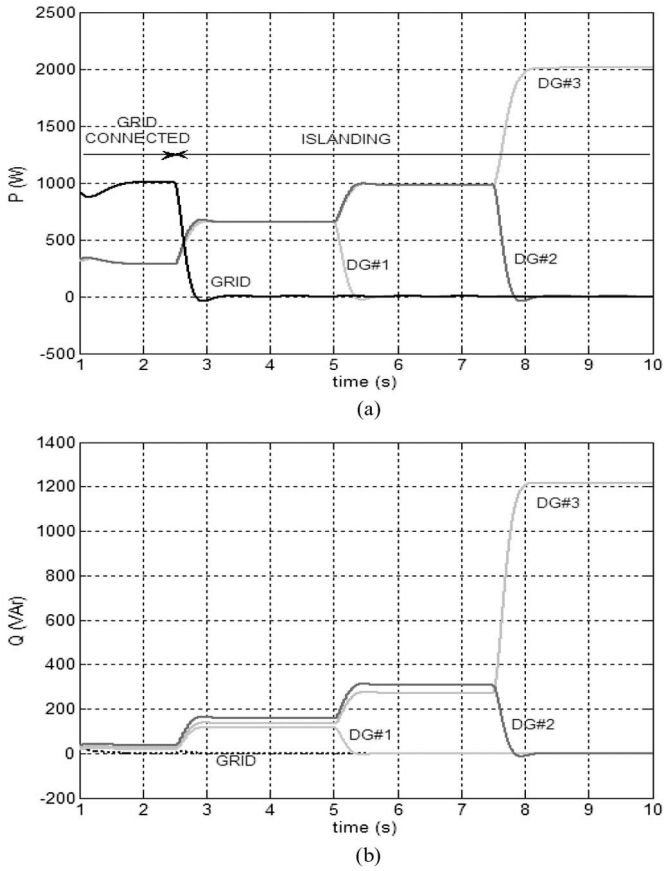

Fig. 15. Transient response of a two-inverter ac MG. (a) Active power and (b) reactive power.

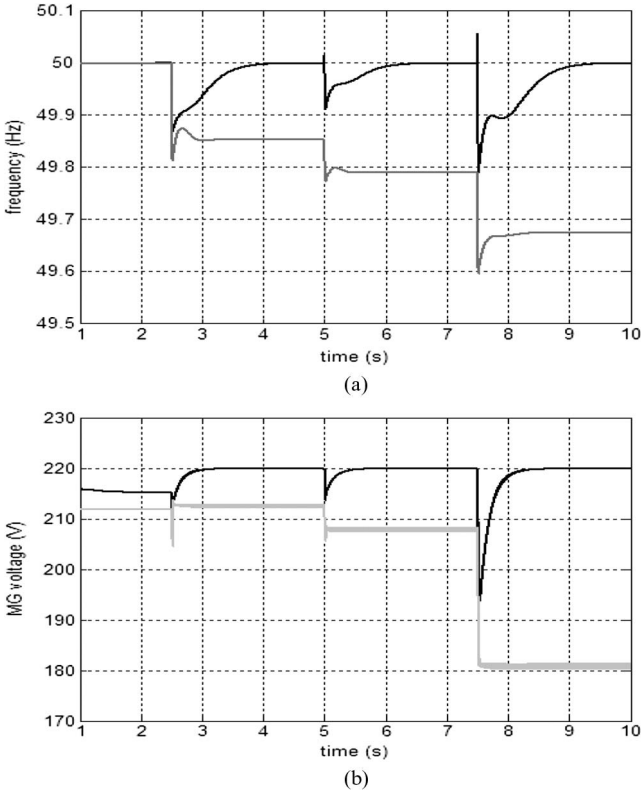

Fig. 16. (a) Frequency and (b) voltage rms transient response of the ac MG (gray line) without and (black line) with the secondary control.

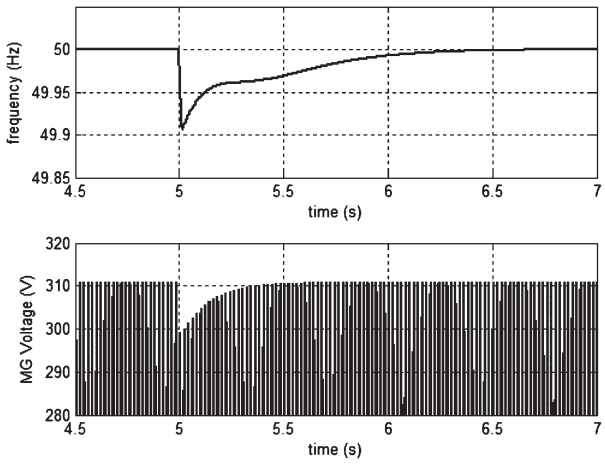

Fig. 17. Detail of the frequency and amplitude restorations.

by the secondary-control loops. Fig. 16(a) and (b) shows, respectively, the frequency- and amplitude-restoration action done by the secondary control. Note that these control loops avoid the inherent steady-state error produced by the primary control (detailed waveforms are shown in Fig. 17).

Fig. 18 shows the transient response of the frequency and amplitude of the ac MG for a nonplanned islanded scenario that occurred at $t = 2.5$ s. After 1 s, the islanding operation is detected, the tertiary-control loops are disabled, and the frequency and amplitude references for the secondary control are self-generated. Notice that the small transient frequency deviation can be used to detect that the ac MG is operating in islanded mode. This transient barely affects the performance of the MG system.

Fig. 19 shows the active- and reactive-power flow from the grid to the MG. In this case, the three inverters remained connected to the grid, and the tertiary control changed the reference of the active power while keeping the reactive power equal to zero in steady state.

Finally, Fig. 20 shows the P dynamics during different scenarios: At $t = 0$ s, the MG is in islanded mode; after the synchronization process, at $t = 5$ s, the MG is connected to the grid; and at $t = 10$ s, the reference of P is changed from zero to 1 kW. Fig. 21 shows a detail of the voltage difference between the MG and the grid during the synchronization process, showing the action of the synchronization loop. Consequently, the operation during island and grid-connected modes, as well as the transitions between modes and its corresponding synchronization process, has been performed successfully.

IV. Hierarchical Control of DC MGs

There are several problems associated with ac MGs, such us the need for synchronization of the distributed generators, the inrush currents due to transformers, reactive-power flow, harmonic currents, and three-phase unbalances. Furthermore, there is an increasing interest to integrate prime movers with dc output, such as PV modules, fuel cells, and dc energy-storage systems like batteries, supercapacitor modules, or hydrolysers [39]–[43]. This section deals with the hierarchical

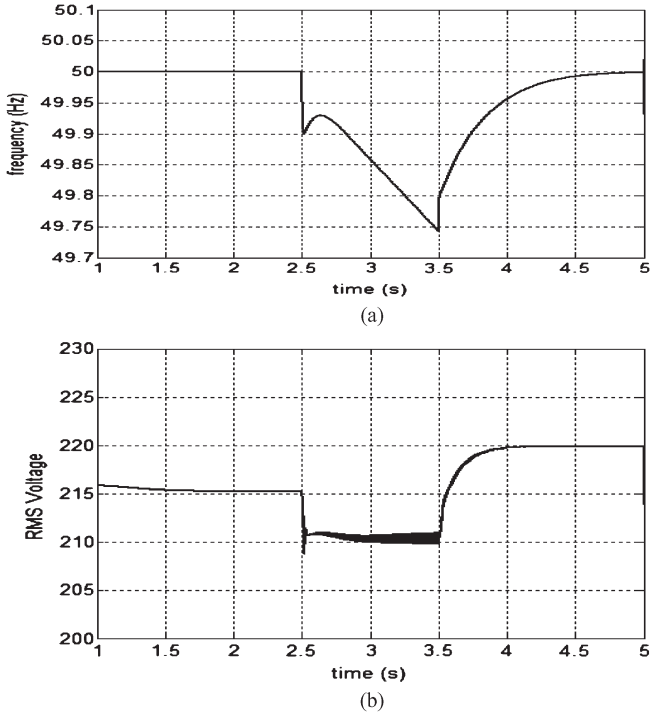

Fig. 18. Islanding detection for a nonplanned islanded scenario. Transient response of the (a) frequency and (b) amplitude.

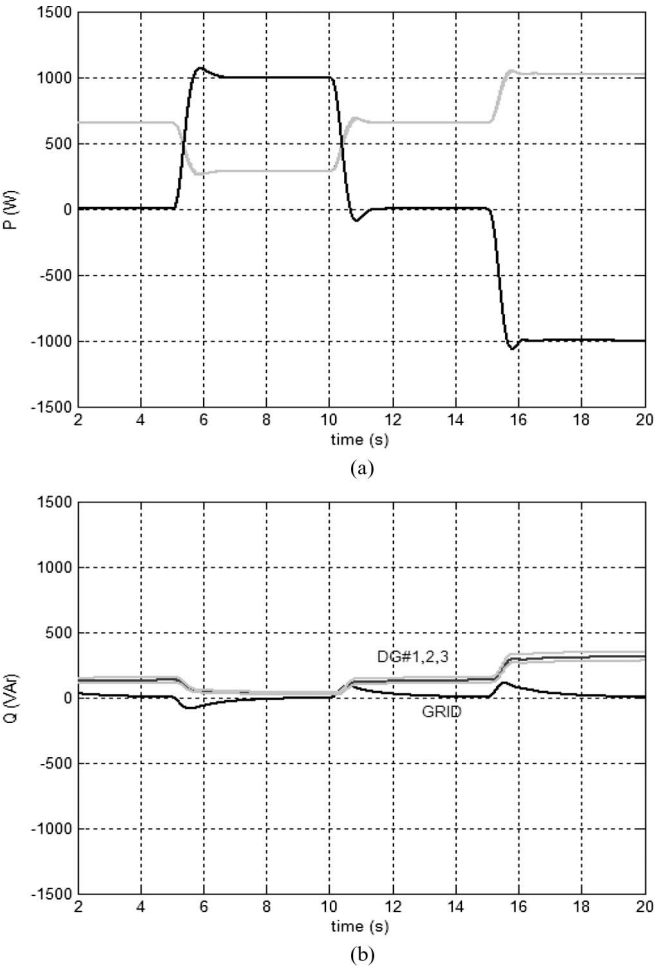

Fig. 19. Tertiary control: (a) active power and (b) reactive power.

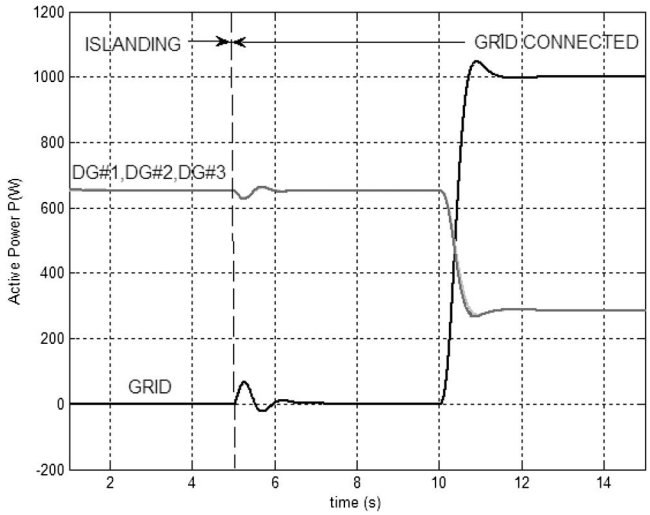

Fig. 20. Transfer process from islanding to grid-connected mode.

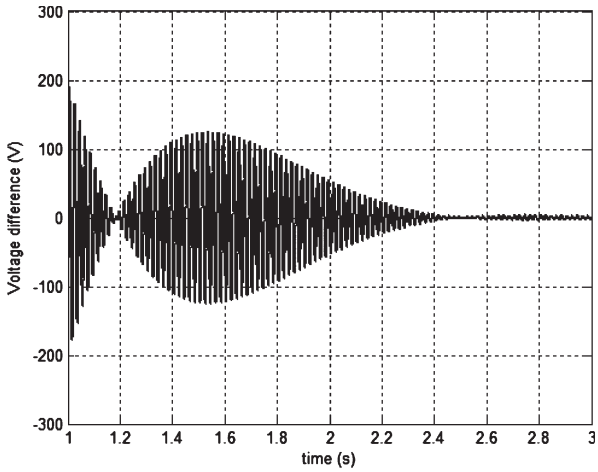

Fig. 21. Detail of the voltage difference between the grid and the MG during the synchronization process.

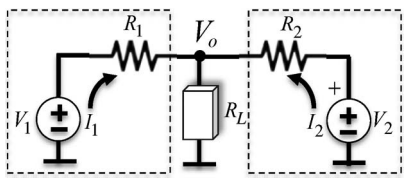

Fig. 22. Equivalent circuit of two parallel-connected dc power supplies.

control of dc MGs consisting of the following three control levels, similarly conceived as with the ac MG. In this case, the control structure is easier to perform as follows. The primary control consists of a resistive virtual output-impedance loop, integrating the soft-start approach. The secondary control is based on an external common controller to restore the voltage deviation inside the dc MG. The tertiary control regulates the current flow from/to an external stiff dc source, which can be, for instance, a dc distribution system or dc/ac converter connected to the grid or an ac MG part.

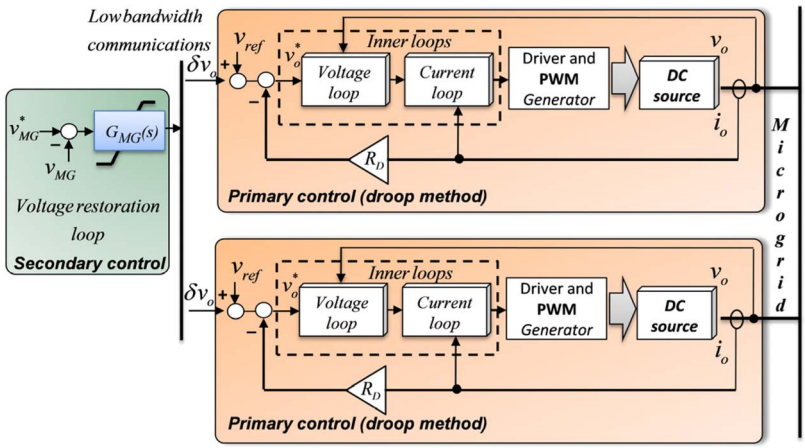

Fig. 23. Primary and secondary controls of a dc MG.

A. Primary Control

Fig. 22 shows the equivalent circuit of two dc power supplies connected in parallel sharing a common load through resistive output impedances. If there is some voltage difference, this will circulate a current between both dc sources. In order to reduce the circulating current, we can program virtual output impedances by using a primary control. This control level adjusts the voltage reference provided to the inner current and voltage control loops (level 0). It includes the virtual output-impedance loop in which the output voltage can be expressed as [44]:

$$v_o^* = v_{\text{ref}} - R_D \cdot i_o \tag{17}$$

where i_o is the output current, R_D is the virtual output impedance, and v_{ref} is the output voltage reference at no load. Assuming that ε_v is the maximum allowed voltage deviation, R_D and v_{ref} must be designed as follows:

$$v_{\text{ref}} = v_n - \varepsilon_v/2 \tag{18}$$

$$R_D = \varepsilon_v/i_{\max} \tag{19}$$

with v_n being the nominal output voltage and $i_{\max}$ as the maximum output current.

This control loop provides resistive output impedance to the power converters to compensate for the difference between the voltage references $\Delta v_o^* = v_{o1}^* - v_{o2}^*$. Thus, the current sharing between the two converters $\Delta i_o = i_{o1} - i_{o2}$ (see Fig. 19) can be expressed as follows:

$$\Delta i_o = \Delta v_o^*/R_D. \tag{20}$$

This control loop not only allows parallel operation of the converters but also improves the dynamic performance of the output voltage. However, it has the inherent load-dependent voltage deviation.

B. Secondary Control

To solve the problem of the voltage deviation, a secondary control is proposed. The voltage level in the MG v_{MG} is sensed and compared with the voltage reference v_{MG}^*, and the error processed through a compensator is sent to all the units δv_o to restore the output voltage (see Fig. 23). The controller can be expressed as follows:

$$\delta v_o = k_p\,(v_{\text{MG}}^* - v_{\text{MG}}) + k_i \int (v_{\text{MG}}^* - v_{\text{MG}})\,dt \tag{21}$$

k_p and k_i being the control parameters of the secondary-control compensator. Notice that δv_o must be limited in order not to exceed the maximum voltage deviation. Finally, (17) becomes

$$v_o^* = v_{\text{ref}} + \delta v_o - R_D \cdot i_o. \tag{22}$$

In order to connect the MG to a dc stiff source, first, we have to measure the voltage of this stiff source, and that will be the reference of the secondary control loop. After the transient, the MG can be connected to the dc stiff source through the static bypass switch. At that moment, the MG does not have any exchange of power with the external dc source.

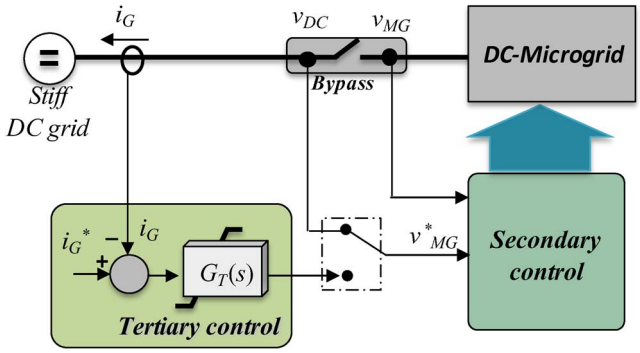

Fig. 24. Tertiary control and synchronization loop of a dc MG.

C. Tertiary Control

Once the MG is connected to the dc source, the power flow can be controlled by changing the voltage inside the MG. As can be seen in Fig. 24, by measuring the current (or the power) through the static bypass switch i_G, it can be compared with the desired positive or negative current i_G^* (or power), depending whether we want to import or export energy.

TABLE II
DC MG CONTROL-SYSTEM PARAMETERS

Parameter	Symbol	Value	Units
Primary Control			
Virtual Impedance	R_D	2	Ω
Secondary Control			
Proportional term	k_p	1	-
Integral term	k_i	5000	s^{-1}
Tertiary Control			
Proportional term	k_p'	10	V/A
Integral term	k_i'	3000	V/As

The controller can be expressed as follows:

$$\delta v_o = k_p' \left(i_G^* - i_G\right) + k_i' \int \left(i_G^* - i_G\right) dt \qquad (23)$$

where k_p' and k_i' are the control parameters of the tertiary-control compensator. Here, δv_o is also saturated in case of being outside the limits of $\pm\varepsilon_v$. Notice that, depending on the sign of I_G^*, the power flow can be exported $(I_G^* > 0)$ or imported $(I_G^* < 0)$.

D. Results

Simulation results of two dc/dc buck converters connected in parallel, forming a dc-MG, are presented in order to show the feasibility of the proposed hierarchical control. The MG voltage was selected at 400 V, the control was implemented by using voltage and current loops, and the virtual output impedance was rated at 2 Ω. The selected control parameters are listed in Table II.

Fig. 25 shows a set of waveforms derived from the use of the different levels of the proposed control scheme. In all of them, at 8 ms, the primary control was activated, and at 15 ms, there is a sudden step of the load. Fig. 25(a) shows the voltage droop caused by the primary control. Notice that an increase of the current produces higher voltage droop.

Fig. 25(b) shows the effect of the secondary control, which compensates for the voltage deviations caused by the primary control. Finally, Fig. 25(c) shows the action of the tertiary control, which regulates the current flow to/from a stiff dc source connected to the MG. Note that at 17 ms, a reference of 20 A is imposed by this controller, producing a voltage deviation inside the voltage reference to inject the desired current to the dc stiff grid.

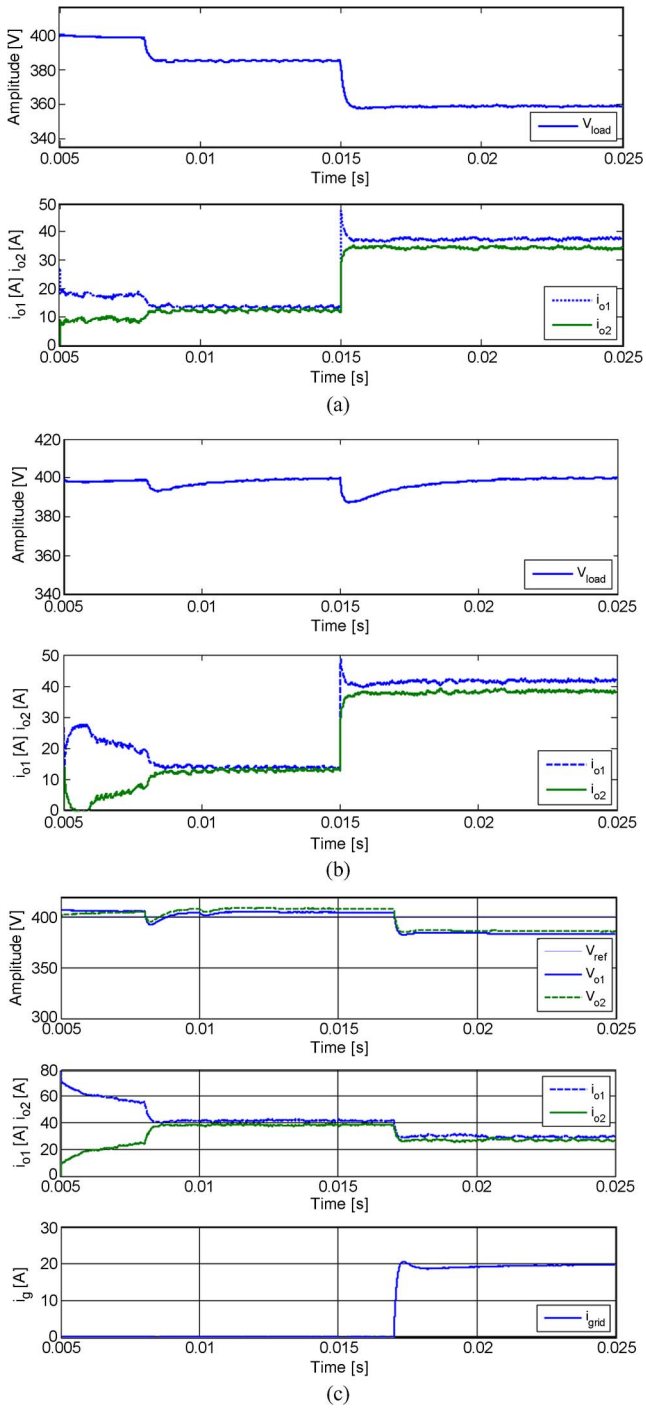

Fig. 25. Behavior of the voltage and currents of the dc MG by using (a) primary, (b) secondary, and (c) tertiary control.

V. CONCLUSION AND FUTURE TRENDS

This paper has presented a general approach of hierarchical control for MGs. The hierarchical control stems from ISA-95. A three-level control is applied to ac and dc MGs. On the one hand, the control of ac MG mimics a large-scale power system ac grid, pointing out the similarities between both systems. On the other hand, the hierarchical control of dc MGs presents novel features that can be useful in distributed power systems applications, such as telecommunication dc-voltage networks, among others.

Consequently, flexible MGs are obtained which can be used fully for ac or dc interconnection with an ac or dc distribution system, controlling the power flow from the MG to these systems. In addition, these MGs are able to operate in both island or stiff-source-connected modes, as well as to achieve a seamless transfer from one mode to the other.

By using the proposed approach, as shown Fig. 26, a multi-MG cluster can be performed, constituting an SG. In this sense, the tertiary control could provide high-level inertias to interconnect more MGs, thus acting as the primary control of the cluster. In this sense, MGs will behave like a voltage source

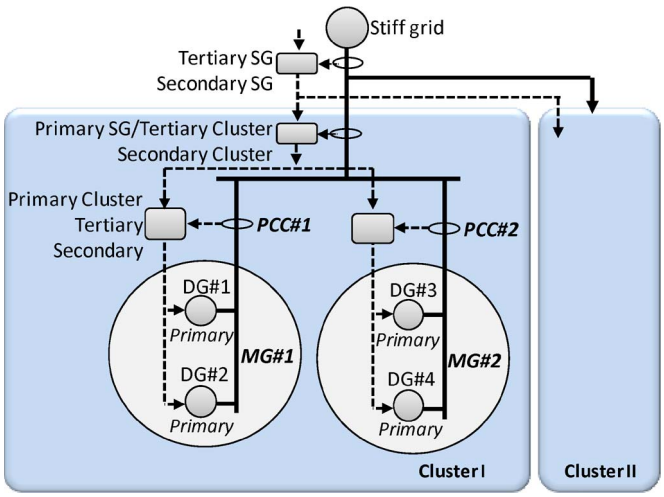

Fig. 26. Clusters of multiple MGs forming an SG configuration.

with high inertias. Thus, a superior control level could send all the references to each cluster of MGs to restore the frequency and amplitude, i.e., the secondary control of the cluster level. Finally, the tertiary cluster control can fix the active and reactive power to be provided by this cluster or act like a primary control to interconnect more clusters. As a result, we could scale the hierarchy of control as necessary.

Using this approach, the system turns more flexible and expandable, and consequently, it could integrate more and more MGs without changing the local hierarchical control system associated to each MG.

REFERENCES

[1] H. Farhangi, "The path of the smart grid," *IEEE Power Energy Mag.*, vol. 8, no. 1, pp. 18–28, Jan./Feb. 2010.

[2] M. Mahmoodi, R. Noroozian, G. B. Gharehpetian, and M. Abedi, "A suitable power transfer control system for interconnection converter of DC microgrids," in *Proc. ICREPQ Conf.*, 2007, pp. 223.1–223.7.

[3] Release 2 Y. Rebours and D. Kirschen, A survey of definitions and specifications of reserve services2005, Oct..

[4] Y. Ito, Y. Zhongqing, and H. Akagi, "DC micro-grid based distribution power generation system," in *Proc. IEEE IPEMC*, 2004, vol. 3, pp. 1740–1745.

[5] H. Kakigano, Y. Miura, T. Ise, and R. Uchida, "DC micro-grid for super high quality distribution—System configuration and control of distributed generations and energy storage devices," in *Proc. IEEE IPEMC*, 2004, vol. 3, pp. 1740–1745.

[6] H. Jiayi, J. Chuanwen, and X. Rong, "A review on distributed energy resources and MicroGrid," *Renew. Sustain. Energy Rev.*, vol. 12, no. 9, pp. 2472–2483, Dec. 2008.

[7] "Technical paper—Definition of a set of requirements to generating units," in *UCTE*, 2008.

[8] H. Kakigano, Y. Miura, T. Ise, and R. Uchida, "DC micro-grid for super high quality distribution—System configuration and control of distributed generations and energy storage devices," in *Proc. 37th IEEE PESC*, Jun. 2006, pp. 1–7.

[9] D. Salomonsson, L. Soder, and A. Sannino, "An adaptive control system for a dc microgrid for data centers," in *Conf. Rec. 42nd IEEE IAS Annu. Meeting*, 2007, pp. 2414–2421.

[10] J. Bryan, R. Duke, and S. Round, "Decentralized generator scheduling in a nanogrid using dc bus signaling," in *Proc. IEEE Power Eng. Soc. Gen. Meet.*, 2004, pp. 977–982.

[11] P. Viczel, "Power electronic converters in dc microgrid," in *Proc. IEEE 5th Int. CPE*, 2007, pp. 1–6.

[12] P. Kundur, *Power System Stability and Control*. New York: McGraw-Hill, 1994.

[13] E. C. W. de Jong and P. T. M. Vaessen, *DC Power Distribution for Server Farms*. Nijmegen, The Netherlands: KEMA Consulting, Sep. 2007.

[14] J. M. Guerrero, J. C. Vasquez, J. Matas, M. Castilla, and L. G. de Vicuna, "Control strategy for flexible microgrid based on parallel line-interactive UPS systems," *IEEE Trans. Ind. Electron.*, vol. 56, no. 3, pp. 726–736, Mar. 2009.

[15] J. M. Guerrero, J. Matas, L. Garcia de Vicuna, M. Castilla, and J. Miret, "Decentralized control for parallel operation of distributed generation inverters using resistive output impedance," *IEEE Trans. Ind. Electron.*, vol. 54, no. 2, pp. 994–1004, Apr. 2007.

[16] J. M. Guerrero, J. Matas, L. G. de Vicuna, M. Castilla, and J. Miret, "Wireless-control strategy for parallel operation of distributed-generation inverters," *IEEE Trans. Ind. Electron.*, vol. 53, no. 5, pp. 1461–1470, Oct. 2006.

[17] J. M. Guerrero, L. Garcia de Vicuna, J. Matas, M. Castilla, and J. Miret, "Output impedance design of parallel-connected UPS inverters with wireless load-sharing control," *IEEE Trans. Ind. Electron.*, vol. 52, no. 4, pp. 1126–1135, Aug. 2005.

[18] J. M. Guerrero, L. G. de Vicuna, J. Matas, M. Castilla, and J. Miret, "A wireless controller to enhance dynamic performance of parallel inverters in distributed generation systems," *IEEE Trans. Power Electron.*, vol. 19, no. 5, pp. 1205–1213, Sep. 2004.

[19] J. C. Vasquez, J. M. Guerrero, M. Liserre, and A. Mastromauro, "Voltage support provided by a droop-controlled multifunctional inverter," *IEEE Trans. Ind. Electron.*, vol. 56, no. 11, pp. 4510–4519, Nov. 2009.

[20] K. Alanne and A. Saari, "Distributed energy generation and sustainable development," *Renew. Sustain. Energy Rev.*, vol. 10, no. 6, pp. 539–558, Dec. 2006.

[21] R. H. Lasseter, A. Akhil, C. Marnay, J. Stevens, J. Dagle, R. Guttromson, A. S. Meliopoulous, R. Yinger, and J. Eto, "White paper on integration of distributed energy resources. The CERTS microgrid concept," in *Proc. Consortium Elect. Reliab. Technol. Solutions*, Apr. 2002, pp. 1–27.

[22] P. L. Villeneuve, "Concerns generated by islanding," *IEEE Power Energy Mag.*, vol. 2, no. 3, pp. 49–53, May/Jun. 2004.

[23] M. C. Chandorkar and D. M. Divan, "Control of parallel operating inverters in standalone ac supply system," *IEEE Trans. Ind. Appl.*, vol. 29, no. 1, pp. 136–143, Jan./Feb. 1993.

[24] C. C. Hua, K. A. Liao, and J. R. Lin, "Parallel operation of inverters for distributed photovoltaic power supply system," in *Proc. IEEE PESC Conf.*, 2002, pp. 1979–1983.

[25] R. Ambrosio and S.E. Widergren, "A framework for addressing interoperability issues," in *Proc. IEEE PES Gen. Meet.*, Tampa, FL, Jun. 2007, pp. 1–5.

[26] S. L. Hamilton, E. W. Gunther, R. V. Drummond, and S. E. Widergren, "Interoperability—A key element for the grid and DER of the future," in *Proc. IEEE PES Transmiss. Distrib.*, 2006, pp. 927–931.

[27] A. A. Salam, A. Mohamed, and M. A. Hannan, "Technical challenges on microgrids," *ARPN J. Eng. Appl. Sci.*, vol. 3, no. 6, pp. 64–69, Dec. 2008.

[28] B. Kroposki, T. Basso, and R. DeBlasio, "Microgrid standards and technologies," in *Proc. IEEE PES Gen. Meet.*, 2009, pp. 1–4.

[29] G. Suter and T. G. Werner, "The distributed control centre in a smartgrid," in *Proc. CIRED*, 2009, pp. 1–4.

[30] K. Visscher and S. W de Haan, "Virtual synchronous machines (VSG's) for frequency stabilisation in future grids with significant share of decentralized generation," in *Proc. CIRED*, 2008, pp. 1–4.

[31] Q.-C. Zhong and G. Weiss, "Static synchronous generators for distributed generation and renewable energy," in *Proc. IEEE PES/PSCE*, 2009, pp. 1–6.

[32] K. Visscher and S. W. H. De Haan, "Virtual synchronous machines (VSG's) for frequency stabilisation in future grids with a significant share of decentralized generation," in *Proc. SmartGrids Distrib., IET-CIRED Semin.*, Jun. 23-24, 2008, pp. 1–4.

[33] A. Madureira, C. Moreira, and J. Peças Lopes, "Secondary load-frequency control for microGrids in islanded operation," in *Proc. ICREPQ*, Frankfurt, Germany, 2005, pp. 1–4.

[34] J. P. Lopes, C. Moreira, and A. G. Madureira, "Defining control strategies for MicroGrids islanded operation," *IEEE Trans. Power Syst.*, vol. 21, no. 2, pp. 916–924, May 2006.

[35] B. Awad, J. Wu, and N. Jenkins, "Control of distributed generation," *Elektrotechnik & Informationstechnik*, vol. 125, no. 12, pp. 409–414, 2008.

[36] A. Mehrizi-Sanir and R. Iravani, "Secondary control for microgrids using potential functions: Modeling issues," in *Proc. CYGRE*, 2009, pp. 182.1–182.9.

[37] K. Vanthournout, K. De Brabandere, E. Haesen, J. Van den Keybus, G. Deconinck, and R. Belmans, "Agora: Distributed tertiary control of distributed resources," in *Proc. 15th Power Syst. Comput. Conf.*, Liege, Belgium, Aug. 22–25, 2005.

[38] A. G. Madureira and J. A. Peças Lopes, "Voltage and reactive power control in MV networks integrating MicroGrids," in *Proc. ICREPQ*, Seville, Spain, 2007.
[39] T. Rigole, K. Vanthournout, and G. Deconinck, "Resilience of distributed microgrid control systems to ICT faults," in *Proc. 19th Int. CIRED*, Vienna, Austria, 2007.
[40] Z. Jiang and X. Yu, "Hybrid DC- and AC-linked microgrids: towards integration of distributed energy resources," in *Proc. IEEE Conf. Global Sustain. Energy Infrastructure*, Atlanta, GA, Nov. 17-18, 2008, pp. 1–8.
[41] R. Nilsen and I. Sorfonn, "Hybrid power generation systems," in *Proc. EPE*, 2009, pp. 1–9.
[42] A. D. Erdogan and M. T. Aydemir, "Use of input power information for load sharing in parallel connected boost converters," *Elect. Eng.*, vol. 91, no. 4/5, pp. 229–250, 2009.
[43] Z. Ye, D. Boroyevich, K. Xing, and F. C. Lee, "Design of parallel sources in DC distributed power systems using gain-scheduling technique," in *Proc. IEEE PESC*, 1999, pp. 161–165.
[44] H. Kakigano, Y. Miura, T. Ise, and R. Uchida, "DC voltage control of the DC micro-grid for super high quality distribution," *IEEJ Trans. Ind. Appl.*, vol. 127, no. 8, pp. 890–897, 2007.
[45] J. Schönberger, R. Duke, and S. D. Round, "DC-bus signaling: A distributed control strategy for a hybrid renewable nanogrid," *IEEE Trans. Ind. Elecron.*, vol. 53, no. 5, pp. 1453–1460, Oct. 2006.
[46] T. Thringer, "Grid-friendly connecting of constant-speed wind turbines using external resistors," *IEEE Trans. Energy Convers.*, vol. 17, no. 4, pp. 537–542, Dec. 2002.
[47] X. Sun, Y.-S. Lee, and D. Xu, "Modeling, analysis, and implementation of parallel multi-inverter systems with instantaneous average-current-sharing scheme," *IEEE Trans. Power Electron.*, vol. 18, no. 3, pp. 844–856, May 2003.
[48] J. M. Guerrero, L. Garcia de Vicuna, and J. Uceda, "Uninterruptible power supply systems provide protection," *IEEE Ind. Electron. Mag.*, vol. 1, no. 1, pp. 28–38, May 2007.
[49] J. M. Guerrero, L. Hang, and J. Uceda, "Control of distributed uninterruptible power supply systems," *IEEE Trans. Ind. Electron.*, vol. 55, no. 8, pp. 2845–2859, Aug. 2008.
[50] J.M. Guerrero and J. Uceda, "Guest Editorial," *IEEE Trans. Ind. Electron.—Special Section on Uninterruptible Power Supply (UPS) Systems*, vol. 55, no. 8, pp. 2842–2844, Aug. 2008.
[51] J. C. Vasquez, J. M. Guerrero, A. Luna, P. Rodriguez, and R. Teodorescu, "Adaptive droop control applied to voltage-source inverters operating in grid-connected and islanded modes," *IEEE Trans. Ind. Electron.*, vol. 56, no. 10, pp. 4088–4096, Oct. 2009.

Josep M. Guerrero (S'01–M'03–SM'08) received the B.S. degree in telecommunications engineering, the M.S. degree in electronics engineering, and the Ph.D. degree in power electronics from the Technical University of Catalonia, Barcelona, Spain, in 1997, 2000, and 2003, respectively.

He is an Associate Professor with the Technical University of Catalonia, where he teaches courses on digital signal processing, control theory, and renewable energy systems. Since 2004, he has been responsible for the Renewable Energy Laboratory, Escola Industrial de Barcelona. His research interests include photovoltaics, wind-energy conversion, uninterruptible power supplies, storage energy systems, and microgrids. He is the Editor-in-Chief of the *International Journal of Integrated Energy Systems*.

Dr. Guerrero is an Associate Editor of the IEEE TRANSACTIONS ON INDUSTRIAL ELECTRONICS and the IEEE TRANSACTIONS ON POWER ELECTRONICS. He has been a Guest Editor of the IEEE TRANSACTIONS ON INDUSTRIAL ELECTRONICS for the Special Section: "Uninterruptible Power Supply (UPS) Systems," and of the IEEE TRANSACTIONS ON POWER ELECTRONICS for the Special Issues: "Power Electronics for Wind Energy Conversion" and "Power Electronics for Microgrids." He is involved on several IEEE Industrial Electronics Society (IES) Committees, and he usually chairs and organizes sessions in IES and PELS conferences. Currently, he chairs the IEEE IES Technical Committee on Renewable Energy Systems.

Juan C. Vasquez received the B.S. degree in electronics engineering from the Universidad Autonoma de Manizales, Manizales, Colombia, in 2004 and the Ph.D. degree from the Department of Automatic Control Systems and Computer Engineering, Technical University of Catalonia, Barcelona, Spain, in 2009.

He was an Assistant Professor with the Universidad Autonoma de Manizales, where he taught courses on digital circuits, servo systems, and flexible manufacturing systems. He is currently a Postdoctoral Research Assistant with the Department of Automatic Control Systems and Computer Engineering, Technical University of Catalonia, where he teaches courses on renewable-energy systems. His research interests include modeling, simulation, and power management applied to distributed generation in microgrids.

José Matas received the B.S., M.S., and Ph.D. degrees in telecommunications engineering from the Technical University of Catalonia, Barcelona, Spain, in 1988, 1996, and 2003, respectively.

From 1988 to 1990, he was an Engineer with a consumer electronics company. Since 1990, he has been an Associate Professor with the Department of Electronic Engineering, Technical University of Catalonia, Vilanova i la Geltrú, Spain. His research interests include power-factor-correction circuits, active-power filters, uninterruptible power systems, distributed power systems, and nonlinear control.

Luis García de Vicuña received the Ingeniero de Telecomunicación and Dr.Ing. degrees from the Technical University of Catalonia, Barcelona, Spain, in 1980 and 1990, respectively, and the Dr.Sci. degree from Université Paul Sabatier, Toulouse, France, in 1992.

From 1980 to 1982, he was an Engineer with a control applications company. He is currently an Associate Professor with the Department of Electronic Engineering, Technical University of Catalonia, Vilanova i la Geltrú, Spain, where he teaches courses on power electronics. His research interests include power-electronic modeling, simulation and control, active-power filtering, and high-power-factor ac/dc conversion.

Miguel Castilla received the B.S., M.S., and Ph.D. degrees in telecommunication engineering from the Technical University of Catalonia, Barcelona, Spain, in 1988, 1995, and 1998, respectively.

Since 2002, he has been an Associate Professor with the Department of Electronic Engineering, Technical University of Catalonia, Vilanova i la Geltrú, Spain, where he teaches courses on analog circuits and power electronics. His research interests are in the areas of power electronics, nonlinear control, and renewable-energy systems.